



Publication Year	2019
Acceptance in OA	2020-12-21T08:29:45Z
Title	A 2.3-8.2 GHz room temperature multi-channel receiver for phased array feed application
Authors	NAVARRINI, Alessandro, SCALAMBRA, ALESSANDRO, RUSTICELLI, SIMONE, MACCAFERRI, ANDREA, CATTANI, ALESSANDRO, PERINI, FEDERICO, ORTU, Pierluigi, RODA, JURI, MARONGIU, Pasqualino, SABA, Andrea, POLONI, MARCO, LADU, Adelaide
Publisher's version (DOI)	10.1109/UKRCON.2019.8879848
Handle	http://hdl.handle.net/20.500.12386/29027

A 2.3-8.2 GHz Room Temperature Multi-Channel Receiver for Phased Array Feed Application

A. Navarrini¹, A. Scalambra², S. Rusticelli², A. Maccaferri², A. Cattani², F. Perini², P. Ortu¹, J. Roda², P. Marongiu¹, A. Saba^{1,3}, M. Poloni², A. Ladu¹

¹INAF (National Institute for Astrophysics)-Astronomical Observatory of Cagliari, Selargius, Italy
alessandro.navarrini@inaf.it, pierluigi.ortu@inaf.it, pasqualino.marongiu@inaf.it, adelaide.ladu@inaf.it

²INAF (National Institute for Astrophysics)-Institute of Radio Astronomy, Bologna, Italy
a.scalambra@ira.inaf.it, s.rusticelli@ira.inaf.it, a.maccaferri@ira.inaf.it, a.cattani@ira.inaf.it, f.perini@ira.inaf.it

³ASI (Italian Space Agency), Rome, Italy, andrea.saba@asi.it

Abstract—We describe the design, fabrication and test results of a multi-channel heterodyne receiver operating at room temperature across the 2.3-8.2 GHz Radio Frequency (RF) band. Such a “Warm Section” (WS) receiver is part of a Phased Array Feed (PAF) demonstrator that is being built for radio astronomy application. The WS receiver is cascaded to the PAF cryogenic section that incorporates an antenna array with low noise pre-amplification stages. The WS receiver consists of four rack-mountable modules, each of which can process eight RF inputs. Four modules are arranged in a standard 19” rack to allow handling a total of 32 RF signals. The modules perform filtering (through four-way switch filter bank) and down-conversion (to the 375-650 MHz IF band). The IF signals are converted to optical through analogue Wavelength Division Multiplexing IFoF (IF over fiber) transmitters incorporated into the WS receiver. The signals are sent through optical fibers to a backend, where they are converted back to IF before digitization by an Analog-to-Digital Unit.

Keywords—receiver, phased array feed, heterodyne, filter bank, fiber-optic link, radio astronomy

I. INTRODUCTION

High-sensitivity large-scale surveys are an essential tool for new discoveries in radio astronomy. A Phased Array Feed placed at the focal plane of an antenna can increase the Field-of-View (FoV) and the mapping efficiency by fully sampling the sky. Multiple beams can be formed by adding signals from electrically small focal plane radiating elements of the array using different sets of complex weights.

PHAROS (PHased Arrays for Reflector Observing Systems) [1]-[2] is a cryogenically cooled PAF demonstrator based on an array of dual-polarization 10×11 Vivaldi antennas designed for radio astronomy observation across the 4-8 GHz band. The array is shown in Fig. 1 along with its RF transparent plexiglas vacuum window (thickness ≈15 mm). The instrument upgraded version PHAROS2 [3] utilizes new components to reduce the system noise temperature, enhance the aperture efficiency and digitize the signals from a sub-array of 24 active antenna elements of the PAF that synthesize four independent single-polarization beams.

In this paper, we describe the design and experimental results of the 2.3-8.2 GHz WS 32-channel receiver we developed for PHAROS2. Only 24 of the 32 WS channels will be used. In section II, we illustrate the PHAROS2 system diagram and the multi-channel receiver specifications. The receiver design and architecture is discussed in section III. The fabrication, integration,

assembly and characterization of the receiver are presented in section IV.

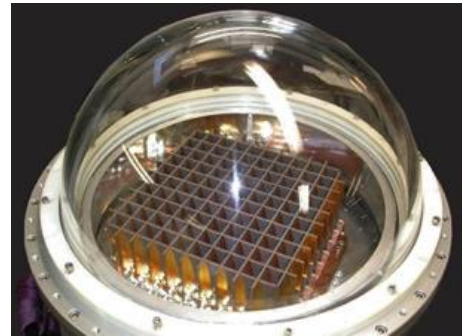


Fig. 1 PHAROS2 focal plane array and dome-shaped vacuum window attached to the cryostat.

II. PHAROS2 SYSTEM DIAGRAM AND WS SPECIFICATIONS

A block diagram of the PHAROS2 phased array feed is illustrated in Fig. 2. The PAF features the following: a) a 4-8 GHz cryogenic section comprising an array of 10×11 Vivaldi antennas cascaded with low-noise amplifiers; b) a 2.3-8.2 GHz room-temperature “Warm Section” multi-channel receiver; c) an FPGA-based Italian Tile Processing Module (iTPM) digital backend capable of digitizing and forming four independent beams across a ≈275 MHz IF band [4]. The main specifications of the Warm Section receiver are listed in Table 1. The instrument is required to handle up to 32 RF input signals, of which only 24 will be used for PHAROS2.

III. DESIGN OF WARM SECTION MULTI-CHANNEL RECEIVER

A 3D view of the WS 32-channel receiver, equipped with all its modules, is given in Fig. 3. The WS includes four eight-channel WS RF/IF modules, one LO distribution module and one WS monitor and control module arranged in a standard 6U×19-inch rack. The receiver performs signal filtering by switched filter bank, signal conditioning, and single frequency down-conversion of a section of the 2.3-8.2 GHz RF band down to the 375-650 MHz IF band (275 MHz instantaneous bandwidth). The downconversion scheme utilizes sideband separating mixers in LSB (Lower Side Band) with USB (Upper Side Band) internally terminated. The IF signals are converted to optical signals by analogue WDM (Wavelength Division Multiplexing) “IFoF” (IF over fiber) fiber-optic transmitter (OTX) that transports two IFs over a single optical fiber. One of the four BPF filters, BPF-A, is specified to cover the broad 2.3-8.2 GHz RF frequency band, while the other three filters (BPF-B, -C and -D) have ≈275 MHz “narrowband”

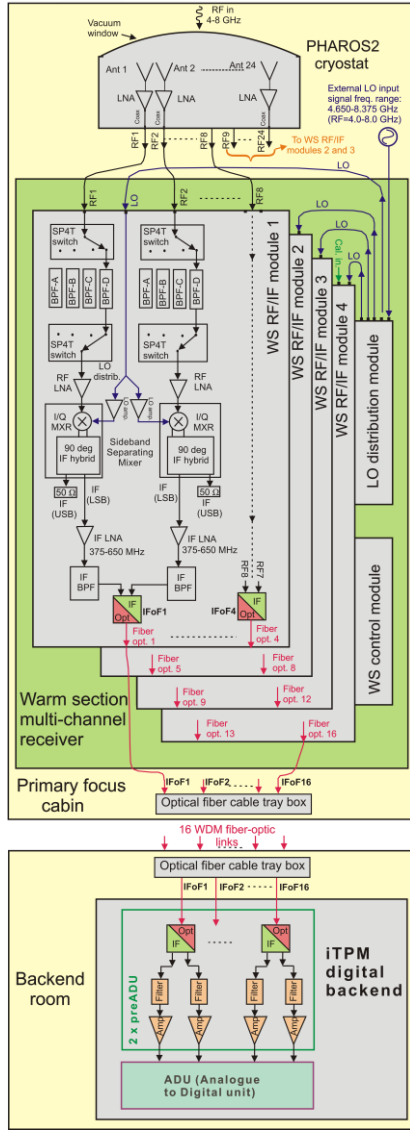


Fig. 2. Block diagram of the PAF receiver chain showing the PHAROS2 cryostat (top), the Warm Section multi-channel receiver (middle) and the iTPM digital backend (bottom). The schematic of the Warm Section multi-channel receiver, located in the primary focus receiver room, is enclosed by the green background rectangle.

TABLE I WARM SECTION MULTI-CHANNEL SPECIFICATIONS

Number of RF channels	32 (four \times eight-channel RF/IF modules)
RF band	2.3-8.2 GHz
Frequency conversion scheme	Sideband Separating Mixer in LSB (USB terminated)
LO band	2.950-8.575 GHz
IF band	375-650 MHz
Switched Filter Banks: Band Pass Filter frequency range and LO frequency	<i>BPF-A</i> : 2.300-8.200 GHz; LO tuning $f_{LO}=2.950-8.575$ GHz <i>BPF-B</i> : 4.775-5.050 GHz; $f_{LO}=5.425$ GHz <i>BPF-C</i> : 5.780-6.055 GHz; $f_{LO}=6.430$ GHz <i>BPF-D</i> : 6.445-6.720 GHz; $f_{LO}=7.095$ GHz
Signal transportation	Two IF output signals transported over a single optical fiber (IFoF) using WDM
Number of WDM fiber-optics link	16
Control module	Optical fiber-Ethernet mediaconverter and microcontroller for BPF selection and LO power and PCB temperature monitoring

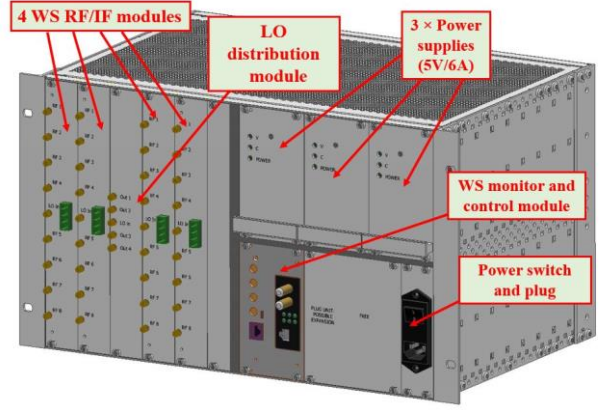


Fig. 3. Design of PHAROS2 Warm Section multi-channel receiver.

features, with bands centered around astronomical lines. The selection of one of the narrowband filters allows to achieve an image sideband rejection greater than 50 dB.

We note that the frequency range of the WS receiver (2.3-8.2 GHz) is larger than the one delivered by the cryogenic section (4-8 GHz). Therefore, the room-temperature Front-End (and associated digital backend) can be used not only for application with the PHAROS2 cryogenic array, but also with other PAF antenna array that could be developed to cover the band 2.3-8.2 GHz ($f_{max}/f_{min}=3.4$) or part of it.

A. Eight-channel Warm Section RF/IF module

Each of the WS RF/IF modules (Fig. 4) includes a PCB circuit and four WDM fiber-optic transmitters (“OTXs”) on opposite sides respect to a mechanical support. The RF/IF module has eight SMA RF input connectors, one SMA LO input connector (centered on the front panel) and one quad LC/APC output connector to extract the four WDM IFoF optical fiber outputs provided by the four OTXs. Fig. 5 shows a schematic of the receiver chain implemented with the board. The module employs a single four-layer PCB based on Rogers RG4003C substrate with thickness 0.508 mm and commercial surface-mounted components that are soldered in place (no bonding required). The PCB adopts the standard double-height Eurocard size (6U, equivalent to ≈ 233.35 mm) that can be plugged into a standard chassis, which in turn can be mounted in a 19-inch rack. Views of the board PCB layers are shown in Fig. 5. The board and its components (switches, RF and IF LNAs, mixers, etc.) are easy to fabricate and assemble; it is biased with a single voltage (+5 V) and incorporate a sensor for monitoring the physical temperature. The eight channels of the module adopt identical components and same-length transmission lines to achieve similar performance. The IF output signals are extracted from MCX connectors mounted orthogonal to the board. Eight 16.5 cm long coaxial cables (type RG316), connectorized with male MCX connectors on both sides, are employed to connect the board IFs to the input of the WDM fiber-optics transmitters.

The PCB has one SMA connector for the LO input signal, centrally located on the RF side of the board. The LO signal is amplified, band pass filtered (by a cascade of low pass and high pass filters) and distributed internally to the PCB with one eight-way splitter based on a cascade of

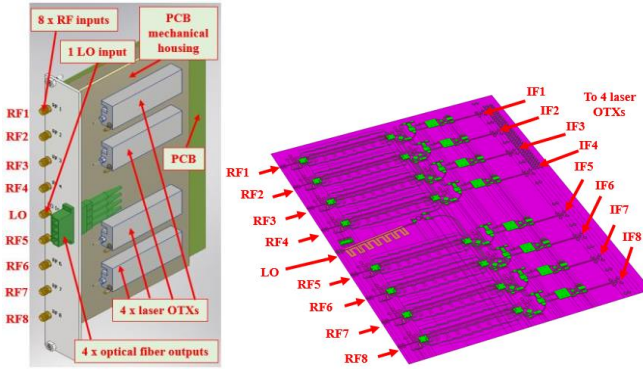


Fig. 4. Left panel: Design of the WS RF/IF module showing the eight RF inputs, the LO input, the quad LC/APC fiber-optics connector, the PCB and its mechanical housing (left panel). Right panel: Design of the PCB with RF, LO and IF components. The size of the PCB is 160 mm×233.35 mm.

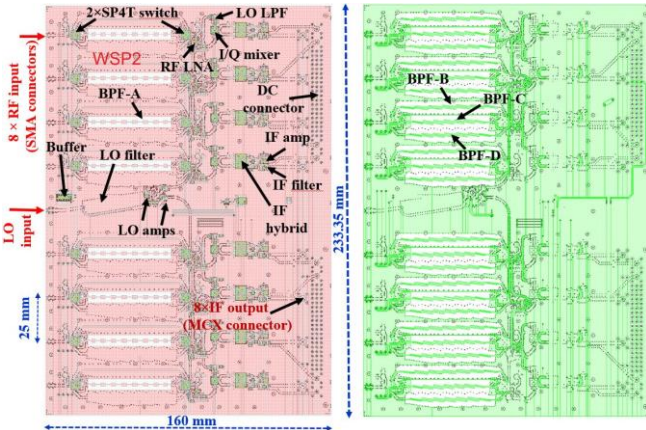


Fig. 5. WS RF/IF board design. View of two different PCB layers. Left: top metallization layer with components showing the BPF-A layer. Right: metallization layer n. 3, showing the BPF-B, BPF-C and BPF-D.

Wilkinson power dividers. Equal electrical path lengths are used for the LO distribution signal chain to the eight receiver channels of the PCB.

We used the commercial software NI-AWR MicroWave Office to design the PCB circuitry and simulate the electromagnetic response of the WS receiver chains that include band pass filters and components. The S-parameter simulator was employed to optimize the scattering parameters of the receiver chains. Fig. 6 plots the simulated RF transmissions of the four BPFs, which match closely the specified ones in terms of passband (bandwidth at half-power points), insertion loss, return loss, in-band ripple, stop-band attenuations and size.

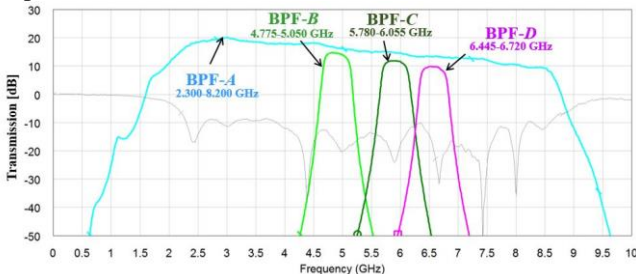


Fig. 6. Electromagnetic simulation of the $|S_{21}|$ transmission of one WS RF/IF board receiver chain from SMA board input to mixer (includes the RF LNA, BPF and mixer conversion loss).

B. Local Oscillator distribution module

The four WS RF/IF modules receive a copy of the same LO signal from the LO distribution module (Fig. 3) so that the mixers (eight per board) are pumped under identical conditions. The 2.950-8.575 GHz four-way LO splitter utilizes Wilkinson power dividers and incorporates a directional coupler (coupling value ≈ -20 dB) that directs part of the signal to a detector (AD8317). The detector allows converting the LO power to a decibel-scaled DC output used for monitoring purpose.

C. Warm Section monitor and control module

The WS monitor and control module (Fig. 3) is based on commercial optical fiber to Ethernet mediaconverter (Digitus DN-82010) and microcontroller (Arduino Leonardo ETH) incorporated into a 3U rack-mountable box biased with +5 V. The module utilizes transmitting/receiving mode with TX/RX multimode fiber and has two TTL outputs. It allows selection of one among four possible bandpass filters of the WS RF/IF modules and returns voltage values inversely proportional to the LO power of the LO distribution module. Furthermore, the module reads the physical temperature provided by the four sensors placed on the PCBs (one per board). The front-panel includes LEDs that provide information on the selected filter, the presence of LO power and of bias voltage.

IV. WS RECEIVER FABRICATION, INTEGRATION AND CHARACTERIZATION

The PCBs and the mechanical housings were fabricated, respectively by Italian companies and INAF. Photos of the boards and modules are shown in Fig. 7. The board includes 9 SMA input connectors (8 RFs and 1 LO), 8 MCX output connectors (8 IFs) and two 96-pin DC connectors (DIN 41612C). The four OTXs of each module are bolted to the mechanical housing, which also supports a plastic frame for routing the optical fiber pigtail (length 1 m) to the quad LC/APC connector. The IFoF fiber-optic links were developed for the SKA Low Frequency Aperture Array by an INAF-led collaboration with industrial partners and adopted for this project. The IFoF optical receivers incorporate digital step attenuators (DSA) with 31 dB range and 1 dB step for power level adjustment before the Analog to Digital Unit of the iTPM.

Two identical 32-channel receivers were fully assembled and characterized, although only one was required to equip the PHAROS2 PAF. The eight-channel WS RF/IF modules were characterized at INAF before they were assembled into the two receiver racks. The modules perform well, according to specification, and have similar performance. Below, we present the test results of one of the boards (Board #6).

We characterized the RF/IF modules with and without the IFoF optical links. For receiver characterization without IFoF we extracted the outputs from the on-board MCX IF connectors. For the tests, we utilized a 4-port VNA equipped with calibrated converter measurement capabilities (Keysight N5249A and N5249AU-082). We calibrated out the effects of the coaxial cables from the VNA ports to the WS RF/IF module ports. The test setup is shown in Fig. 8. We connected the Port 3 of the VNA to the board SMA local oscillator input, and Port 1 and 2 of the VNA to the SMA RF



Fig. 7. Photos of the WS RF/IF module. Top left: mechanical housing (left) and fabricated PCB (right) before assembly. Microwave absorbers are glued in the pockets of the PCB mechanical housing. Top right: PCB board (first prototype version) and mechanical housing during assembly with optical transmitters. Bottom: Four WS RF/IF modules fully assembled, with OTXs.

input connector and to the MCX IF output connector of the module, respectively. The powers at the board inputs were set to -5 dBm on the LO port and to -30 dBm on the RF port, respectively. We tested the eight channels in turn, one after the other.

Fig. 9 shows an example of the measured receiver gains for the eight channels when the LO is set at a fixed frequency of 5 GHz and the RF is sweeping from 4 to 6 GHz; the broadband band pass filter “BPF-A” was selected. Vertical lines (in red) limit the nominal LSB (4350-4625 MHz) and USB (5375-5650 MHz) that are downconverted to the 375-650 MHz IF band. The receiver signal gain is in the range $G_{LSB}=15-18$ dB across the LSB (signal band) and below $G_{USB}=-6$ dB across the USB (image band). The image sideband rejection, i.e. the ratio between the conversion power gains $IR=G_{LSB}/G_{USB}$ at the available IF port, is greater than 23 dBc across the nominal band.

We repeated the above described tests at 12 different LO frequencies, from 3 GHz to 8.5 GHz by 0.5 GHz steps, and measured the LSB gains of the eight-channels of the eight RF/IF boards. Across 2.3-8.2 GHz the LSB gains are in the range $G_{LSB}=6-23$ dB; these are greater towards the lower part of the RF band (around 2.5 GHz) and fall off at the highest frequencies (beyond ≈ 8.2 GHz). The measured image sideband rejection is in the range $IR=23-60$ dBc. Within the instantaneous 275 MHz IF band covered by the receivers the gain variation are ± 2.5 dB around the average value. The image sideband rejection with BPF-A has minima $IR \approx 20$ dBc at the center of the IF band (≈ 510 MHz) and reaches values greater than 40 dBc (up to 60 dBc) towards the IF band edges (at 375 MHz and 650 MHz).

Selecting the narrow band filters (BPF-B, BPF-C and BPF-D) allows to operate the receiver channels with much improved performance: test results show that the LSB signal gain and image sideband rejections of the WS receiver modules without optical link are in the range $G_{LSB}=9-13$ dB and $IR > 50$ dBc, respectively. Within the 275 MHz band covered by the receivers the gain variation are ± 1 dB around the average value. The much improved sideband rejection results from the combined effect of the mixer sideband separation and of the filter rejection.

We tested the WS receiver with IFoF link. The average gain across the PHAROS2 4-8 GHz band is $G_{LSB} \approx 50$ dB with optical receiver digital step attenuator set to $DSA=25$ dB. The gain can be varied from ≈ 45 dB to ≈ 75 dB by changing the DSA from 31 dB to its 0 dB minimum attenuation.

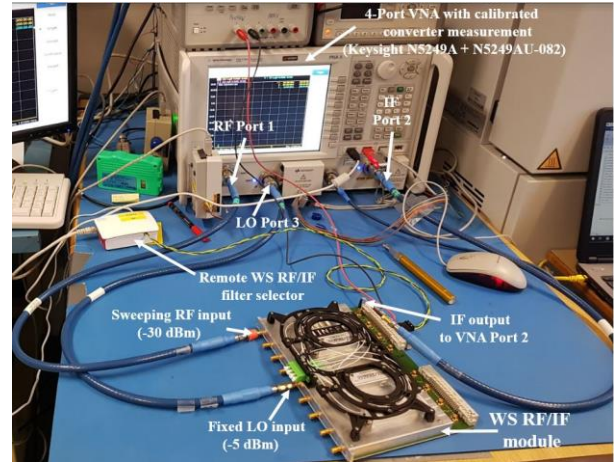


Fig. 8. Testing of one of the WS RF/IF boards (without the IFoF links). The RF port of the VNA is connected to channel 1 of the board. The IF signal is extracted from the board MCX connector corresponding to the channel 1 RF input.

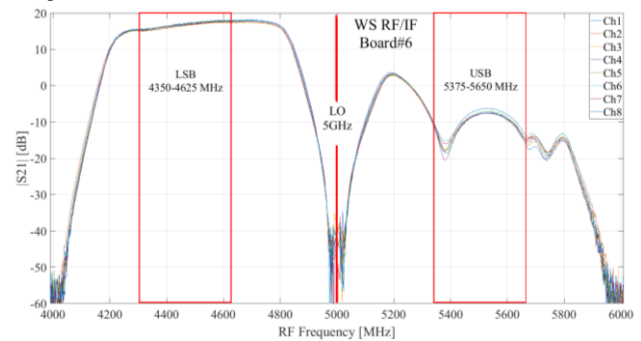


Fig. 9. VNA measured transmissions of the eight channels of one of the WS RF/IF boards by selecting filter BPF-A and LO frequency 5 GHz.

REFERENCES

- [1] J. Simons, M. Ivashina, J. G. b. d. Vaate, and N. Roddis, "Beamformer system model of focal plane arrays in deep dish radio telescopes," European Radar Conf. EURAD 2005, Paris, France, 3-4 October 2005.
- [2] L. Liu, K. Grainge, and A. Navarrini, "Analysis of Vivaldi array antenna for phased array feeds application," IEEE MTT-S Int. Conf. on Num. Elec. and Multiph. Mod. and Opt. for RF, Micr., and THz App. (NEMO), Seville, Spain, 17-19 May, 2017.
- [3] A. Navarrini, J. Monari, A. Scalambra, A. Melis, R. Concu, G. Naldi, A. Maccaferri, A. Cattani, P. Ortu, J. Roda, F. Perini, G. Comoretto, M. Morsiani, A. Ladu, S. Rusticelli, A. Mattana, P. Marongiu, A. Saba, M. Schiaffino, E. Carretti, F. Schillirò, E. Urru, G. Pupillo, M. Poloni, T. Pisanu, R. Nesti, G. Muntoni, K. Zarb Adami, A. Magro, R. Chiello, L. Liu, K. Grainge, M. Keith, M. Pantaleev, W. van Cappellen, "Design of PHAROS2 Phased Array Feed," Proc. of 2nd URSI Atl. Radio Sci. Meet. (AT-RASC), Gran Canaria, Spain, 28 May – 1 June 2018.
- [4] G. Naldi, G. Comoretto, R. Chiello, S. Pastore, G. Pupillo, A. Mattana, A. Melis, R. Concu, M. Alderighi, A. Aminaei, J. Baker, C. Belli, S. Chiarucci, S. D'Angelo, G. Dalle Mura, A. De Marco, R. Halsall, A. Magro, J. Monari, A. Navarrini, F. Perini, M. Poloni, M. Roberts, S. Rusticelli, M. Schiaffino, F. Schillirò, E. Zaccaro, K. Zarb Adami, "Development of a new digital signal processing platform for the Square Kilometer Array." Proc. of 2nd URSI Atl. Radio Sci. Meet. (AT-RASC), Gran Canaria, Spain, 28 May – 1 June 2018.